Research Article

SURFACE and INTERFACE ANALYSIS

Received: 29 April 2010 Revised: 17 June 2010 Accepted: 18 June 2010 Published online in Wiley Interscience:

(www.interscience.wiley.com) DOI 10.1002/sia.3670

Characterization and electric field dependence of *N*,*N*′-bis(9H-fluoren-9-ylidene)benzene-1, 4-diamine thin film/substrate interface

Hongliang Xin, Zhuomin Li, Tianxian He and Wenli Deng*

***N*,*N*′-bis(9H-fluoren-9-ylidene)benzene-1,4-diamine deposited onto highly oriented pyrolytic graphite (HOPG) was investigated by contact angle measurement(CAM), Raman spectroscopy and tunneling spectroscopy. The results of CAM and Raman spectra have confirmed that organic layers had deposited on substrate. Tunneling spectra obtained in the scanning tunneling microscopy measurement system were reported as a function of electrode potential. The tunneling current data were acquired at different electrode–electrode separations and depicted significant trend under the action of electric field. Under weak electric fields, the electrode–electrode separation has little effect on the potential of conductance peak. However, with the shrinkage of electrode–electrode separation, the electron transport model obeys the Ohmic law. Copyright © 2010 John Wiley & Sons, Ltd.**

Keywords: electron transfer; electrode–electrode distance; electric field dependence

Introduction

The fluorene family has attracted more and more attention due to its extensive applications. These compounds are commonly used in organic lasers,[1] organic semiconductors,[2] photovoltaic cells[3] and organic light-emitting diode (OLED).[4] Two fluoren-9-ylidene moieties were connected as substituent on the linking benzene ring to form the entire chiral molecule.[5] Diimines derivatives from p-phenylenediamine and 9-fluorenone have been prepared to study the methodologies of imine synthesis.[6] In order to investigate the spatial relationship between two fluoren-9-ylidene units and central aromatic ring, *N*,*N*′-Bis (9H-fluoren-9-ylidene) benzene-1, 4-diamine compound was synthesized.[7]

Scanning tunneling spectroscopy has been used as a powerful tool to investigate charge transfer through molecule–substrate contact.[8] Molecule–substrate contact is key to the molecular electronic devices, such as light-emitting diodes and field-effect transistors.[9] A useful approach to fabricate multilayer nanostructures is forming self assembled monolayer on Au (111) by using the double-end functional molecule, in which Ag-dithiol-Au multilayer structures were built by adsorbing silver ions from solution onto the surfaces of SAMs of dithiols on Au(111).[10] The theoretical[11–15] and experimental[16–23] studies demonstrated that changing the distance between the tip and monolayer might change the Orbital Mediated Tunneling (OMT) peak positions. Distance-dependent current-voltage curves obtained from chemical vapor deposit (CVD) diamond films have been interpreted by tip field-induced band bending at the semiconductor.[18] Scanning tunneling spectroscopic studies have been performed on the Si-terminated 6H-SiC (0001) surface.[18] The distinct bands of empty and filled states at large tip–substrate distances were exhibited. However, the spectra became completely featureless in the range of small tip–substrate distance. A model for the tunneling process had been proposed to explain the distance dependence.[11,14] The local field at molecule differs significantly with the applied sample bias. The tip–substrate distance dependence in the STM-based OMTS of NiTPP deposited on Au (111) was studied.[23] The result was given that the change of tip–substrate distance less than several angstroms produced no measurable changes in orbital energy splitting. However, an undetermined small but persistent shift was also observed.

In this study, we report an experimental study of the *N*,*N*′-bis(9H-fluoren-9-ylidene)benzene-1,4-diamine deposited onto **highly oriented pyrolytic graphite** (HOPG) substrate and investigated by the tunneling technology. The electrode–electrode separations were changed by adjusting the setpoint current prior to spectral measurement. Our results indicate that the tunneling spectrum is dependent on both the electrode potential and electrode–electrode distance. The electric field between electrodes plays an important role in tunneling spectroscopy. The result contributes to the molecular electronics and the research of electron tunneling behavior in tunneling junction.

Material and Methods

Materials:

N,*N*′-bis (9H-fluoren-9-ylidene) benzene-1,4-diamine ($C_{32}H_{20}N_2$, BFBD molecule) was synthesized by the acetic acid-assisted Schiff base reaction between 9-fluorenone and o-phenylenediamine.The chemical structure of the compound is shown in Fig. 1. The

* *Correspondence to: Wenli Deng, College of Materials Science and Engineering, South China University of Technology, Guangzhou 510640, China. E-mail: wldeng@scut.edu.cn*

College of Materials Science and Engineering, South China University of Technology, Guangzhou 510640, China

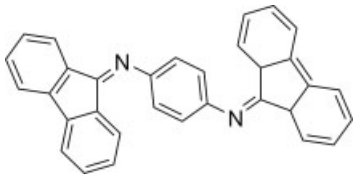

Figure 1. The chemical structure of N,N′-bis(9H-fluoren-9- ylidene) benzene-1,4- diamine molecule.

synthesized product and its structure were confirmed by the melting point measurement, mass spectrum (MS), infrared spectrum (IR), Raman spectrum, Magnetic Resonance (MR) analysis, and X-ray diffraction (XRD) analysis. HOPG was purchased from SPI Structure Probe Inc. (West Chester, PA USA).

Contact angle measurements

Water contact angle was measured with a contact angle system OCA 40(Data Physics Instruments, Germany). Water drops of 2 µl were contacted with samples and the contact angles were recorded using photographic images. The contact angles here were the average values of five independent measurements.

Acquisition of Raman data

The Raman spectroscopy was carried out on the LabRAM Aramis Spectrometer (HJY Company, France). Raman shift scale was between 100 and 2000 cm^{-1}. The laser frequency was 532 nm, and the Raman spectra data were acquired at room temperature.

Tunneling spectra acquisition

Tunneling spectra measurements were carried out with CSPM4000 scanning probe microscope system under ambient conditions. Tips were made mechanically with Pt/Ir (90 : 10) wire as one electrode. The substrate acted as the other electrode. The uppermost layer of HOPG was peeled off immediately before use. A droplet of sample solution in chloroform was applied on the fresh surface to form the molecular film. The concentration of solution was 2×10^{-3} mol/l. Spectroscopy was performed by measuring the tunneling current as a function of electrode potential at fixed electrode–electrode separation (feedback off).

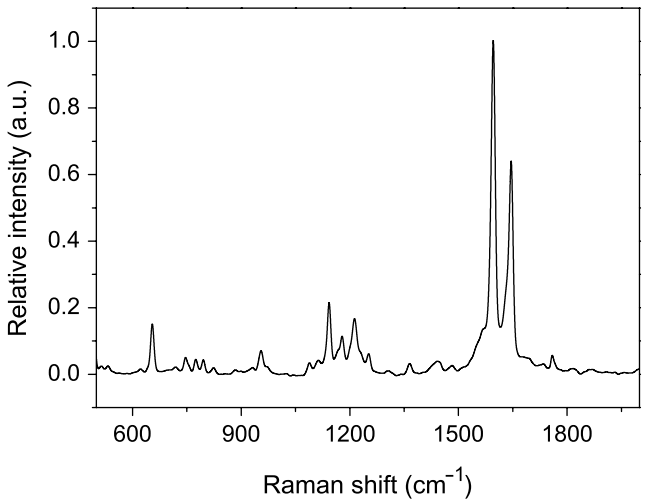

Figure 3. The typical Raman spectra of BFBD. Laser with wavelength 532 nm was used. The intensity has been normalized to the highest intensity of Raman band.

The method of measuring the spectroscopy curve has been reported.[23] The spectroscopy data were acquired with a fixed tip-substrate separation determined by the selected bias voltage and set current. The electrode potential was ramped from −1 to +1 V. During this ramp, the spectroscopy curves were acquired at 512 points with a dwell time of about 200 µs per point. Then the bias and the setpoint were reset to re-establish the feedback loop. All the spectra were acquired at the temperature of about 298 K.

Results and Discussion

Figure 2 shows the changes in water wettability of fresh substrate and the sample deposited on the substrate. The water contact angle of pure substrate is about 45°. After deposition of sample on substrate, the contact angle approached 90°. The difference results from the change of densely packed array structure on substrate surface after deposition of sample.[24]

Figure 3 shows the typical Raman spectra of the compound. This spectrum was obtained with the excitation wavelength $\lambda = 532$ nm. The Raman spectrum is mainly composed of nine

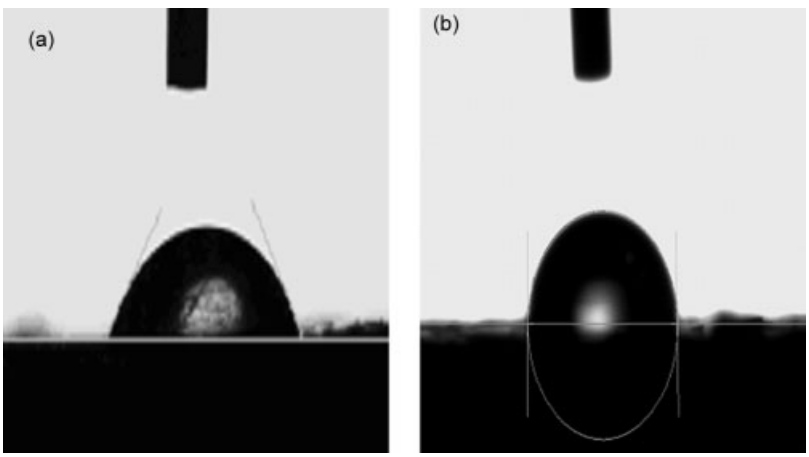

Figure 2. View of the water contact angle: (a) directly on the substrate surface; (b) on the layers of BFBD.

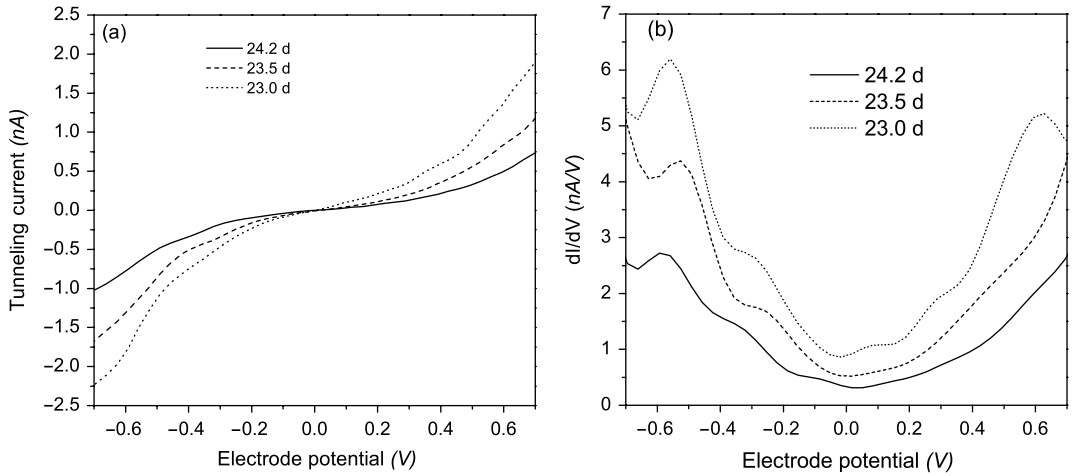

Figure 4. (a) The tunneling current; and (b)the differential current curves at weak electric field.

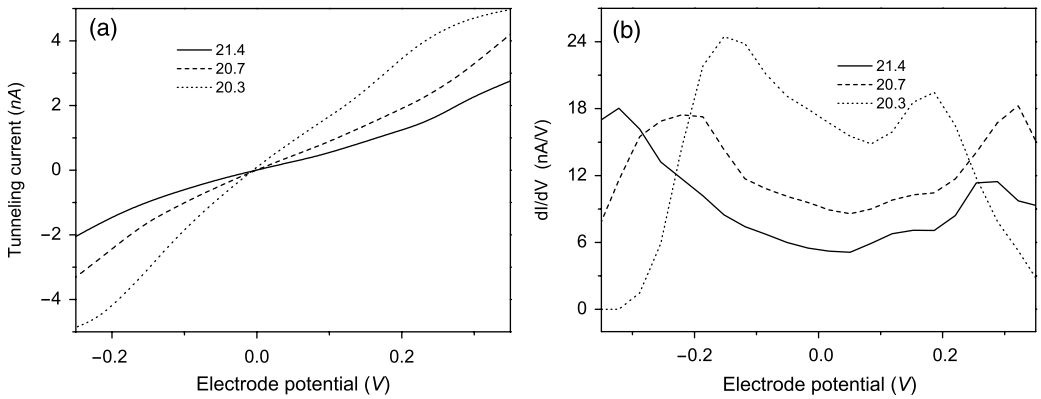

Figure 5. (a) The tunneling current; and (b)the differential current curves at medium electric field.

bands peaked at 1600, 1655, 500, 170, 664, 1153, 1224, 966 and 1039 cm^{-1}. The main band appears at 1600 cm^{-1} is assigned to the C–C stretching vibration of the phenyl ring. The bands at 1153 and 1224 cm^{-1} are related to the C–H bending vibration and the symmetric C–N stretching vibration.[25] The results of Raman experiments demonstrated that the thin film of organic layer was formed on the substrate.

The tunneling current curves and conductance curves obtained at different electrode–electrode separations are presented in Figs 4–6. The distance was changed by resetting the setpoint prior to measurement.

In order to interpret the difference of current curve and conductance with various electrode–electrode separations and find the electron transport mechanism through BFBD molecule, it is necessary to divide the electric field derived from measurement system into three parts which are: weak, medium and strong electric fields, respectively. The following model is introduced to give the detaila of electron transport mechanism.

The discussion is assumed that the positive bias is applied to the substrate. The electron configuration of carbon is $1s^2 2s^2 2p_x^1 2p_y^1$, and that of nitrogen is $1s^2 2s^2 2p_x^1 2p_y^1 2p_z^1$. The formation of BFBD molecule causes the element of nitrogen as lone pair. The lone pair is confined in nitrogen atom. When the positive bias is applied to the substrate, the BFBD layers are exposed to the electric field. Under the action of Coulomb force in electric field, the lone pair of nitrogen atom plays an important role in the transportation of electron from fluorene plane to substrate. According to the strength, the electric fields may be treated as three cases: weak, medium and strong fields, respectively.

When the electrode–electrode distance is large enough, the electric field between electrodes is small. In this case, the BFBD molecule is polarized and the harmonic oscillator is formed under the action of electric field. Figure 4(a) and (b) show the tunneling and differential current of the organic thin film under weak electric field. Some special potential may be found and the peaks of dI/dV curves occurred at these voltages. According to the quantum mechanics theory of harmonic oscillator,[26] the possible energy Eigen values of Hamiltonian can be described. There is only little electron transport when the electrode potential is small and the electronic energy at some special electrode potential may come into resonance with the harmonic oscillator energy level. Thus, several peaks at special potential can be observed going with the increase of electrode potential. Under the case of weak electric field, the electrode–electrode separations are so large that the change of electric field between electrodes can be neglected. The change of distance has little effect on the potential where the peak of differential current curve occurs. These results were consonant with the previous report.[23]

With the decrease of electrode–electrode separation, the maximum of electric field between the electrodes is increased along the scanning potential. The positions of the peak shift toward lower potential with the shrinkage of electrode–electrode

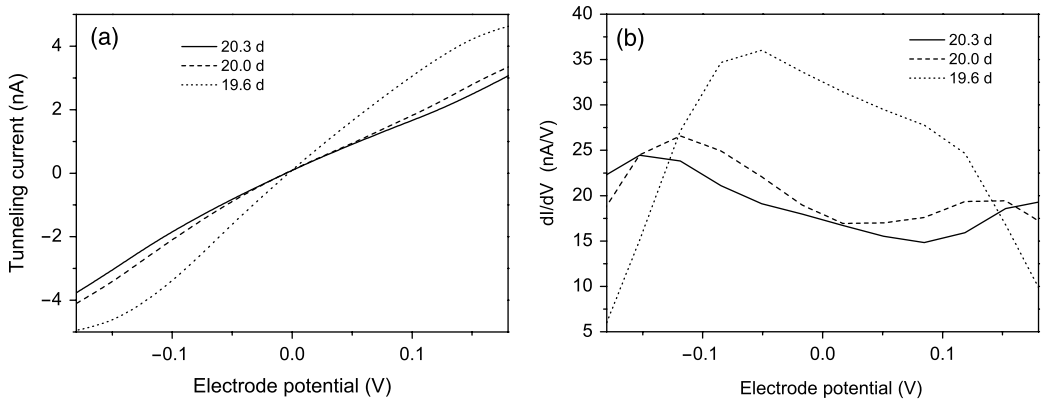

Figure 6. (a) The tunneling current; and (b)the differential current curves at strong electric field.

separation, the trend is shown in Fig. 5. That is because the distance is so small that the trivial shrinkage of electrode–electrode may lead to the striking increase of electric field that cannot be neglected. Under the effect of electric field, the peak potential decreases with the shrinkage of electrode–electrode distance. With further shrinkage of the electrode–electrode separation, the electric field is large enough to delocalize the confined electron and capture the electron from electrode, the electrons can transport through the organic molecule even in very small electrode potential. The BFBD molecule acts as a conductor and reveals metallic-like I-V curves. The current curve acquired at the setpoint current 3 nA is the typical electron transportation under strong electric field. The corresponding current curves and differential current curves are shown in Fig. 6.

The classical theory of electron transfer could be employed to interpret the tunneling behavior, and the electron transfer rate is given:[27]

$$k_{et} = \frac{2\pi}{\hbar} |V_{ts}|^2 \sum_{v_t} \sum_{v_s} P(\varepsilon_t(v_t)) \, |\langle v_t | v_s \rangle|^2 \, \delta(\varepsilon_s(v_s) - \varepsilon_t(v_t) + E_{st}) \quad (1)$$

where V_{ts} is the coupling between electronic states of tips and that of substrate. In Eqn (1), v_t and v_s denote nuclear states of tips and substrate, P is the Boltzmann distribution over donor states, $\varepsilon_t(v_t)$ and $\varepsilon_s(v_s)$ are nuclear energies above the corresponding electronic origins, and E_{st} is the electronic energy gap between the tips and substrate states. Considered the tunneling process, the electron transfer rate is found to decrease exponentially with the tip–substrate distance

$$k_{et} = k_0 e^{-\beta r} \quad (2)$$

where β is the range parameter that characterizes the distance dependence of the electron transfer rate, r is the distance between the electrodes and k_0 is a constant unrelated to r. The tunneling current is proportionate to the electron transfer rate k_{et} and can be described as

$$I_{set} = \alpha k_{et} = \alpha k_0 e^{-\beta r} \quad (3)$$

where I_{set} is the tunneling current determining the electrode–electrode distance, α is a constant factor that determines the relation between tunneling currents and electrode–electrode distances.

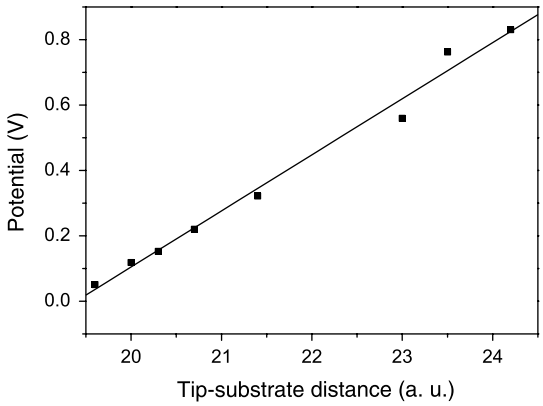

Figure 7. The potential of the differential current peak vs the field dependence.

The potential is determined by both the electrode potential and the distance between electrodes, and can be described as

$$V = \int E \bullet dr = -\frac{E}{\beta \lg e} \lg I_{set} + \frac{E \lg(\alpha k_0)}{\beta \lg e} \quad (4)$$

where V is the potential that caused the electric field E under special electrode–electrode distance adjusted by the setpoint current I_{set}. Owing to the transmission, function is increased exponentially with the shrinkage of electrode–electrode separations,[27,28] the same results can be drawn from Landauer theory.

Figure 7 depicts the potential dependence on electrode–electrode distance. The potential leads to the maximum of differential current. The electrode–electrode distance is determined by Eqn (3). The slope of line in Fig. 7 is proportionate to the electric field depicted in Eqn (4). The curve demonstrates that the electric field in which the differential current reaches the maximum is constant.

Conclusion

From the above discussion, the conclusion can be drawn that the peak of differential current depends not only on the electrode potential, but also on the electric field applied to the organic thin film. The tunneling current curves have different trends under the action of electric field. The conductive model of electrons can be described as harmonic oscillator under weak electric

fields. The electrode–electrode separation has little effect on the potential of conductance peak. However, with the shrinkage of electrode–electrode separation, the electron transport model is metallic-like and the current dependence on electrode potential obeys the Ohmic law.

Acknowledgments

This work was financially supported by the State Key Development Program for Basic Research of China (2009CB930604), and the Natural Science Foundation of Guangdong Province, China (8151064101000111).

References

[1] G. Tsiminis, Y. Wang, P. E. Shaw, A. L. Kanibolotsky, I. F. Perepichka, M. D. Dawson, P. J. Skabara, G. A. Turnbull, D. W. Samuel, *Appl. Phys. Lett.* **2009**, *94*, 243304.
[2] J. Locklin, M. M. Ling, A. Sung, E. R. Mark, Z. Bao, *Adv. Mater.* **2006**, *18*, 2989.
[3] F. Wang, J. Luo, K. Yang, J. Chen, F. Huang, Y. Cao, *Macromolecules* **2005**, *38*, 2253.
[4] K. T. Wong, Y. M. Chen, Y. T. Lin, H. C. Su, C. C. Wu, *Org. Lett.* **2005**, *7*, 5361.
[5] N. M. Glagovich, M. R. Elizabeth, G. Crundwell, J. B. Updegraff, Z. Matthias, A. D. Hunter, *Acta Cryst. E* **2005**, *61*, 01251.
[6] M. E. Taylor, T. L. Fletcher, *J. Org. Chem.* **1956**, *21*, 523.
[7] D. K. Benya, J. F. Freitas, G. Crundwell, N. M. Glagovich, *Acta Cryst. E* **2006**, *62*, 01639.
[8] S. B. Lei, K. Deng, D. L. Yang, Q. D. Zeng, C. Wang, *J. Phys. Chem. B* **2006**, *110*, 1256.
[9] S. R. Forrest, *Chem. Rev.* **1997**, *97*, 1793.
[10] W. Deng, L. Yang, D. Fujita, H. Nejoh, C. Bai, *Appl. Phys. A* **2000**, *71*, 639.
[11] W. Schmickler, *J. Electroanal. Chem.* **1990**, *296*, 283.
[12] A. I. Oniplo, K. F. Berggren, Y. O. Klymenko, L. I. Malysheva, J. J. W. M. Rosink, L. J. Geerligs, E. van der Drift, S. Radelaar, *Phys. Rev. B.* **2000**, *61*, 11118.
[13] M. Plihal, J. W. Gadzuk, *Phys. Rev. B.* **2001**, *63*, 085404.
[14] H. Sumi, *J. Phys. Chem. B* **1998**, *102*, 1833.
[15] J. Zhang, Q. Chi, A. M. Kuznetsov, A. Hansen, H. Wackerbarth, H. E. Christensen, J. Andersen, J. Ulstrup, *J. Phys. Chem. B* **2002**, *106*, 1131.
[16] E. P. Bakkers, Z. Hens, L. P. Kouwenhoven, L. Gurevich, D. Vanmaekelbergh, *Nanotechnology* **2002**, *13*, 258.
[17] D. Katz, O. Millo, S. Kan, U. Banin, *Appl. Phys. Lett.* **2001**, *79*, 117.
[18] S. R. Snyder, H. S. White, *J. Electroanal. Chem.* **1995**, *394*, 177.
[19] V. Gasparov, M. Riehl-Chudoba, M. Schröter, W. Richter *Europhys. Lett.* **2000**, *51*, 527.
[20] W. Han, E. N. Durantini, T. A. Moore, D. Gust, P. Rez, G. Letherman, G. Seely, N. Tao, S. M. Lindsay, *J. Phys. Chem. B* **1997**, *101*, 10719.
[21] Z. Klusek, *Electron. Technol.* **2000**, *33*, 344.
[22] A. D. Muller, F. Muller, M. Hietschold, *Appl. Phys. Lett.* **1999**, *74*, 2963.
[23] W. Deng, K. W. Hipps, *J. Phys. Chem. B* **2003**, *107*, 10736.
[24] X. Miao, A. Gao, S. Hiroto, H. Shinokubo, A. Osuka, H. Xin, W. Deng, *Surf. Interface Anal.* **2009**, *41*, 225.
[25] S. Quillard, G. Louarn, S. Lefrant, *Phys. Rev B* **1994**, *50*, 12496.
[26] P. A. M. Dirac, in *The Principles of Quantum Mechanics*, Oxford University Press, London, **1958**, p. 138.
[27] A. Nitzan, *Annu. Rev. Phys. Chem.* **2001**, *52*, 681.
[28] D. J. Wold, R. Haag, M. A. Rampi, C. D. Frisbie, *J. Phys. Chem. B* **2002**, *106*, 2813.

